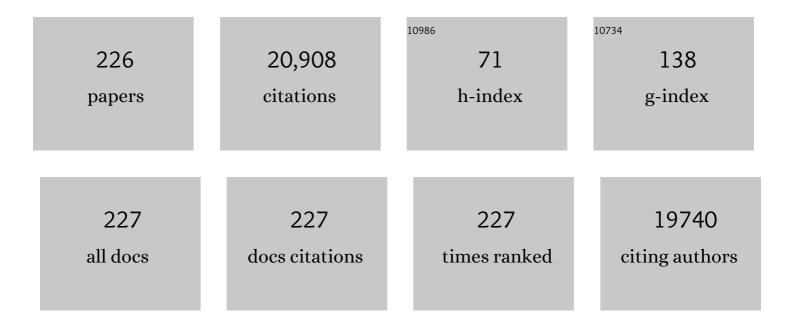
## List of Publications by Year in descending order

Source: https://exaly.com/author-pdf/1017647/publications.pdf Version: 2024-02-01



#	Article	IF	CITATIONS
1	Synthesis, Anion Exchange, and Delamination of Coâ^'Al Layered Double Hydroxide:Â Assembly of the Exfoliated Nanosheet/Polyanion Composite Films and Magneto-Optical Studies. Journal of the American Chemical Society, 2006, 128, 4872-4880.	13.7	1,147
2	Nanosheets of Oxides and Hydroxides: Ultimate 2D Chargeâ€Bearing Functional Crystallites. Advanced Materials, 2010, 22, 5082-5104.	21.0	883
3	Enhancement of the High-Rate Capability of Solid-State Lithium Batteries by Nanoscale Interfacial Modification. Advanced Materials, 2006, 18, 2226-2229.	21.0	739
4	A Superlattice of Alternately Stacked Ni–Fe Hydroxide Nanosheets and Graphene for Efficient Splitting of Water. ACS Nano, 2015, 9, 1977-1984.	14.6	635
5	Selective and Controlled Synthesis of α- and β-Cobalt Hydroxides in Highly Developed Hexagonal Platelets. Journal of the American Chemical Society, 2005, 127, 13869-13874.	13.7	624
6	LiNbO3-coated LiCoO2 as cathode material for all solid-state lithium secondary batteries. Electrochemistry Communications, 2007, 9, 1486-1490.	4.7	620
7	Positively Charged Nanosheets Derived via Total Delamination of Layered Double Hydroxides. Chemistry of Materials, 2005, 17, 4386-4391.	6.7	487
8	Exfoliating layered double hydroxides in formamide: a method to obtain positively charged nanosheets. Journal of Materials Chemistry, 2006, 16, 3809.	6.7	475
9	Large-area graphene-nanomesh/carbon-nanotube hybrid membranes for ionic and molecular nanofiltration. Science, 2019, 364, 1057-1062.	12.6	475
10	Two-Dimensional Oxide and Hydroxide Nanosheets: Controllable High-Quality Exfoliation, Molecular Assembly, and Exploration of Functionality. Accounts of Chemical Research, 2015, 48, 136-143.	15.6	425
11	Hydrogen Uptake in Boron Nitride Nanotubes at Room Temperature. Journal of the American Chemical Society, 2002, 124, 7672-7673.	13.7	424
12	Synthesis and Exfoliation of Co2+â^'Fe3+Layered Double Hydroxides:Â An Innovative Topochemical Approach. Journal of the American Chemical Society, 2007, 129, 5257-5263.	13.7	355
13	Nanotubes of lepidocrocite titanates. Chemical Physics Letters, 2003, 380, 577-582.	2.6	344
14	Topochemical Synthesis, Anion Exchange, and Exfoliation of Coâ^'Ni Layered Double Hydroxides: A Route to Positively Charged Coâ^'Ni Hydroxide Nanosheets with Tunable Composition. Chemistry of Materials, 2010, 22, 371-378.	6.7	323
15	Layered MnO2 Nanobelts: Hydrothermal Synthesis and Electrochemical Measurements. Advanced Materials, 2004, 16, 918-922.	21.0	313
16	Fabrication of aluminum–carbon nanotube composites and their electrical properties. Carbon, 1999, 37, 855-858.	10.3	299
17	Interfacial modification for high-power solid-state lithium batteries. Solid State Ionics, 2008, 179, 1333-1337.	2.7	297
18	Structural Features of Titanate Nanotubes/Nanobelts Revealed by Raman, X-ray Absorption Fine Structure and Electron Diffraction Characterizations. Journal of Physical Chemistry B, 2005, 109, 6210-6214.	2.6	290

# ARTICLE IF CITATIONS Layer-by-Layer Assembly and Spontaneous Flocculation of Oppositely Charged Oxide and Hydroxide Nánosheets into Inorganic Sandwich Layered Materials. Journal of the American Chemical Society, 288 2007, 129, 8000-8007. General Synthesis and Delamination of Highly Crystalline Transition-Metal-Bearing Layered Double 20 3.5 238 Hydroxides. Langmuir, 2007, 23, 861-867. General Synthesis and Structural Evolution of a Layered Family of Ln < sub > 8 < /sub > (OH) < sub > 20 < /sub > Cl < sub > 4 < /sub > A < i>n < /i>H < sub > 2 < /sub > O (Ln = Nd, Sm, Eu, Gd, Tb,) Tj ETQp3171 0.78243414 rgTopochemical Synthesis of Monometallic (Co<sup>2+</sup>–Co<sup>3+</sup>) Layered Double Hydroxide and Its Exfoliation into Positively Charged Co(OH)<sub>2</sub> Nanosheets. Angewandte 22 13.8 215 Chemie - International Edition, 2008, 47, 86-89. Directly Rolling Nanosheets into Nanotubes. Journal of Physical Chemistry B, 2004, 108, 2115-2119. 2.6 A General Strategy to Layered Transitionâ€Metal Hydroxide Nanocones: Tuning the Composition for High Electrochemical Performance. Advanced Materials, 2012, 24, 2148-2153. 24 21.0 209 Topochemical Synthesis of Coâ<sup>^</sup>Fe Layered Double Hydroxides at Varied Fe/Co Ratios: Unique Intercalation of Triiodide and Its Profound Effect. Journal of the American Chemical Society, 2011, 133, 13.7 198 613-620. Tetrahedral Co(II) Coordination in α-Type Cobalt Hydroxide:Â Rietveld Refinement and X-ray Absorption 26 4.0 191 Spectroscopy. Inorganic Chemistry, 2006, 45, 3964-3969. Interface Modulation of Two-Dimensional Superlattices for Efficient Overall Water Splitting. Nano 9.1 191 Letters, 2019, 19, 4518-4526. Layer-by-Layer Assembled Multilayer Films of Titanate Nanotubes, Ag- or Au-Loaded Nanotubes, and 28 Nanotubes/Nanosheets with Polycations. Journal of the American Chemical Society, 2004, 126, 13.7 190 10382-10388. Anion-Exchangeable Layered Materials Based on Rare-Earth Phosphors: Unique Combination of 15.6 184 Rare-Earth Host and Exchangeable Anions. Accounts of Chemical Research, 2010, 43, 1177-1185. Unilamellar Metallic MoS<sub>2</sub>/Graphene Superlattice for Efficient Sodium Storage and 30 17.4 184 Hydrogen Evolution. ACS Energy Letters, 2018, 3, 997-1005. Study of electrochemical capacitors utilizing carbon nanotube electrodes. Journal of Power 7.8 182 Sources, 1999, 84, 126-129. New Layered Rareâ€Earth Hydroxides with Anionâ€Exchange Properties. Chemistry - A European Journal, 32 3.3 173 2008, 14, 9255-9260. Molecularâ€Scale Heteroassembly of Redoxable Hydroxide Nanosheets and Conductive Graphene into 33 21.0 Superlattice Composites for Highâ€Performance Supercapacitors. Advanced Materials, 2014, 26, 4173-4178. Single-layer nanosheets with exceptionally high and anisotropic hydroxyl ion conductivity. Science 34 10.3 154 Advances, 2017, 3, e1602629. Flexible Lithium-Ion Fiber Battery by the Regular Stacking of Two-Dimensional Titanium Oxide 9.1 148 Nanosheets Hybridized with Reduced Graphene Oxide. Nano Letters, 2017, 17, 3543-3549. Synthesis and Delamination of Layered Manganese Oxide Nanobelts. Chemistry of Materials, 2007, 19,

Renzhi

6.7

146

3

6504-6512.

36

#	Article	IF	CITATIONS
37	Growth and Characterization of Iron Oxide Nanorods/Nanobelts Prepared by a Simple Iron–Water Reaction. Small, 2006, 2, 422-427.	10.0	145
38	Engineered Interfaces of Artificial Perovskite Oxide Superlattices <i>via</i> Nanosheet Deposition Process. ACS Nano, 2010, 4, 6673-6680.	14.6	141
39	Constructing Conductive Interfaces between Nickel Oxide Nanocrystals and Polymer Carbon Nitride for Efficient Electrocatalytic Oxygen Evolution Reaction. Advanced Functional Materials, 2019, 29, 1904020.	14.9	140
40	Metal–Organic Framework Hexagonal Nanoplates: Bottom-up Synthesis, Topotactic Transformation, and Efficient Oxygen Evolution Reaction. Journal of the American Chemical Society, 2020, 142, 7317-7321.	13.7	140
41	Development of efficient electrocatalysts via molecular hybridization of NiMn layered double hydroxide nanosheets and graphene. Nanoscale, 2016, 8, 10425-10432.	5.6	134
42	Growth, Morphology, and Structure of Boron Nitride Nanotubes. Chemistry of Materials, 2001, 13, 2965-2971.	6.7	131
43	CVD synthesis of boron nitride nanotubes without metal catalysts. Chemical Physics Letters, 2001, 337, 61-64.	2.6	131
44	Exfoliated Nanosheet Crystallite of Cesium Tungstate with 2D Pyrochlore Structure: Synthesis, Characterization, and Photochromic Properties. ACS Nano, 2008, 2, 1689-1695.	14.6	130
45	Oriented Monolayer Film of Gd <sub>2</sub> O <sub>3</sub> :0.05 Eu Crystallites: Quasiâ€Topotactic Transformation of the Hydroxide Film and Drastic Enhancement of Photoluminescence Properties. Angewandte Chemie - International Edition, 2009, 48, 3846-3849.	13.8	128
46	Gigantic Swelling of Inorganic Layered Materials: A Bridge to Molecularly Thin Two-Dimensional Nanosheets. Journal of the American Chemical Society, 2014, 136, 5491-5500.	13.7	125
47	General Insights into Structural Evolution of Layered Double Hydroxide: Underlying Aspects in Topochemical Transformation from Brucite to Layered Double Hydroxide. Journal of the American Chemical Society, 2012, 134, 19915-19921.	13.7	122
48	Genuine Unilamellar Metal Oxide Nanosheets Confined in a Superlattice-like Structure for Superior Energy Storage. ACS Nano, 2018, 12, 1768-1777.	14.6	122
49	Controllable Fabrication of Amorphous Co—Ni Pyrophosphates for Tuning Electrochemical Performance in Supercapacitors. ACS Applied Materials & Interfaces, 2016, 8, 23114-23121.	8.0	120
50	Shape-Controlled Synthesis and Magnetic Properties of Monodisperse Fe <sub>3</sub> O <sub>4</sub> Nanocubes. Crystal Growth and Design, 2010, 10, 2888-2894.	3.0	113
51	Osmotic Swelling of Layered Compounds as a Route to Producing High-Quality Two-Dimensional Materials. A Comparative Study of Tetramethylammonium versus Tetrabutylammonium Cation in a Lepidocrocite-type Titanate. Chemistry of Materials, 2013, 25, 3137-3146.	6.7	111
52	Two-Dimensional Unilamellar Cation-Deficient Metal Oxide Nanosheet Superlattices for High-Rate Sodium Ion Energy Storage. ACS Nano, 2018, 12, 12337-12346.	14.6	111
53	Synthesis and Properties of Well-Crystallized Layered Rare-Earth Hydroxide Nitrates from Homogeneous Precipitation. Inorganic Chemistry, 2009, 48, 6724-6730.	4.0	110
54	Controlled Synthesis of BN Nanotubes, Nanobamboos, and Nanocables. Advanced Materials, 2002, 14, 366.	21.0	107

#	Article	IF	CITATIONS
55	Monoclinic Tungsten Oxide with {100} Facet Orientation and Tuned Electronic Band Structure for Enhanced Photocatalytic Oxidations. ACS Applied Materials & Interfaces, 2016, 8, 10367-10374.	8.0	106
56	Ln <sub>2</sub> (OH) <sub>4</sub> SO <sub>4</sub> · <i>n</i> H <sub>2</sub> O (Ln = Pr to Tb; <i>n</i> â^¼ 2): A New Family of Layered Rare-Earth Hydroxides Rigidly Pillared by Sulfate Ions. Chemistry of Materials, 2010, 22, 6001-6007.	6.7	104
57	Uniform MgO nanobelts formed from in situ Mg3N2 precursor. Chemical Physics Letters, 2003, 370, 770-773.	2.6	102
58	Colloidal Unilamellar Layers of Tantalum Oxide with Open Channels. Inorganic Chemistry, 2007, 46, 4787-4789.	4.0	99
59	New UVâ€A Photodetector Based on Individual Potassium Niobate Nanowires with High Performance. Advanced Optical Materials, 2014, 2, 771-778.	7.3	97
60	Highly efficient quasi-static water desalination using monolayer graphene oxide/titania hybrid laminates. NPG Asia Materials, 2015, 7, e162-e162.	7.9	94
61	Engineering of carbon and other protective coating layers for stabilizing silicon anode materials. , 2019, 1, 219-245.		94
62	Layered Metal Hydroxides and Their Derivatives: Controllable Synthesis, Chemical Exfoliation, and Electrocatalytic Applications. Advanced Energy Materials, 2020, 10, 1902535.	19.5	90
63	2D Freeâ€Standing Nitrogenâ€Doped Niâ€Ni <sub>3</sub> S <sub>2</sub> @Carbon Nanoplates Derived from Metal–Organic Frameworks for Enhanced Oxygen Evolution Reaction. Small, 2019, 15, e1900348.	10.0	88
64	Multilayer Hybrid Films of Titania Semiconductor Nanosheet and Silver Metal Fabricated via Layer-by-Layer Self-Assembly and Subsequent UV Irradiation. Chemistry of Materials, 2006, 18, 1235-1239.	6.7	86
65	Controllable atomic defect engineering in layered Ni <sub>x</sub> Fe <sub>1â^x</sub> (OH) <sub>2</sub> nanosheets for electrochemical overall water splitting. Journal of Materials Chemistry A, 2021, 9, 14432-14443.	10.3	84
66	All-Nanosheet Ultrathin Capacitors Assembled Layer-by-Layer <i>via</i> Solution-Based Processes. ACS Nano, 2014, 8, 2658-2666.	14.6	82
67	Processing and Performance of Electric Double-Layer Capacitors with Block-Type Carbon Nanotube Electrodes. Bulletin of the Chemical Society of Japan, 1999, 72, 2563-2566.	3.2	80
68	Redox Active Cation Intercalation/Deintercalation in Two-Dimensional Layered MnO <sub>2</sub> Nanostructures for High-Rate Electrochemical Energy Storage. ACS Applied Materials & Interfaces, 2017, 9, 6282-6291.	8.0	80
69	Synthesis of a Solid Solution Series of Layered Eu <sub><i>x</i></sub> Gd <sub>1â<sup>^</sup><i>x</i></sub> (OH) <sub>2.5</sub> Cl <sub>0.5</sub> ·0.9H <sub>2</sub> Cl and Its Transformation into (Eu <sub><i>x</i></sub> Gd <sub>1â<sup>^</sup><i>x</i></sub> ) <sub>2</sub> O <sub>3</sub> with Enhanced	) 4.0	78
70	Photoluminescence Properties. Inorganic Chemistry, 2010, 49, 2960-2968. Nanowires of metal borates. Applied Physics Letters, 2002, 81, 3467-3469.	3.3	76
71	High‥ield Preparation, Versatile Structural Modification, and Properties of Layered Cobalt Hydroxide Nanocones. Advanced Functional Materials, 2014, 24, 4292-4302.	14.9	75
72	Layer-by-Layer Assembly of TaO <sub>3</sub> Nanosheet/Polycation Composite Nanostructures: Multilayer Film, Hollow Sphere, and Its Photocatalytic Activity for Hydrogen Evolution. Chemistry of Materials, 2010, 22, 2582-2587.	6.7	74

#	Article	IF	CITATIONS
73	Tuning the Surface Charge of 2D Oxide Nanosheets and the Bulk-Scale Production of Superlatticelike Composites. Journal of the American Chemical Society, 2015, 137, 2844-2847.	13.7	73
74	Nanometer-thin layered hydroxide platelets of (Y0.95Eu0.05)2(OH)5NO3·xH2O: exfoliation-free synthesis, self-assembly, and the derivation of dense oriented oxide films of high transparency and greatly enhanced luminescence. Journal of Materials Chemistry, 2011, 21, 6903.	6.7	72
75	Recent progress in functionalized layered double hydroxides and their application in efficient electrocatalytic water oxidation. Journal of Energy Chemistry, 2019, 32, 93-104.	12.9	70
76	Coaxial nanocables: Fe nanowires encapsulated in BN nanotubes with intermediate C layers. Chemical Physics Letters, 2001, 350, 1-5.	2.6	69
77	Nanotubes of Magnesium Borate. Angewandte Chemie - International Edition, 2003, 42, 1836-1838.	13.8	69
78	Synthesis of boron nitride nanofibers and measurement of their hydrogen uptake capacity. Applied Physics Letters, 2002, 81, 5225-5227.	3.3	66
79	Investigation on the Growth of Boron Carbide Nanowires. Chemistry of Materials, 2002, 14, 4403-4407.	6.7	66
80	Intrinsic high water/ion selectivity of graphene oxide lamellar membranes in concentration gradient-driven diffusion. Chemical Science, 2016, 7, 6988-6994.	7.4	66
81	Simple Approaches to Quality Large-Scale Tungsten Oxide Nanoneedles. Journal of Physical Chemistry B, 2004, 108, 15572-15577.	2.6	64
82	Two-dimensional organic–inorganic superlattice-like heterostructures for energy storage applications. Energy and Environmental Science, 2020, 13, 4834-4853.	30.8	64
83	Photoluminescence properties of lamellar aggregates of titania nanosheets accommodating rare earth ions. Applied Physics Letters, 2004, 85, 4187-4189.	3.3	63
84	Neat monolayer tiling of molecularly thin two-dimensional materials in 1 min. Science Advances, 2017, 3, e1700414.	10.3	63
85	The effects of extra Li content, synthesis method, sintering temperature on synthesis and electrochemistry of layered LiNi1/3Mn1/3Co1/3O2. Journal of Power Sources, 2006, 162, 629-635.	7.8	57
86	Rare Cobalt-Based Phosphate Nanoribbons with Unique 5-Coordination for Electrocatalytic Water Oxidation. ACS Energy Letters, 2018, 3, 1254-1260.	17.4	57
87	Electrical conductivity and field emission characteristics of hot-pressed sintered carbon nanotubes. Materials Research Bulletin, 1999, 34, 741-747.	5.2	56
88	Highly selective charge-guided ion transport through a hybrid membrane consisting of anionic graphene oxide and cationic hydroxide nanosheet superlattice units. NPG Asia Materials, 2016, 8, e259-e259.	7.9	56
89	Recent advances in developing high-performance nanostructured electrocatalysts based on 3d transition metal elements. Nanoscale Horizons, 2019, 4, 789-808.	8.0	53
90	High purity single crystalline boron carbide nanowires. Chemical Physics Letters, 2002, 364, 314-317.	2.6	52

#	Article	IF	CITATIONS
91	Ni <sub>2</sub> P <sub>2</sub> O <sub>7</sub> Nanoarrays with Decorated C <sub>3</sub> N <sub>4</sub> Nanosheets as Efficient Electrode for Supercapacitors. ACS Applied Energy Materials, 2018, 1, 2016-2023.	5.1	50
92	Spontaneous Direct Band Gap, High Hole Mobility, and Huge Exciton Energy in Atomic-Thin TiO <sub>2</sub> Nanosheet. Chemistry of Materials, 2018, 30, 6449-6457.	6.7	50
93	Potassium niobate nanoscrolls incorporating rhodium hydroxide nanoparticles for photocatalytic hydrogen evolution. Journal of Materials Chemistry, 2008, 18, 5982.	6.7	49
94	Layered materials for supercapacitors and batteries: Applications and challenges. Progress in Materials Science, 2021, 118, 100763.	32.8	48
95	Cobalt-doped Ni–Mn layered double hydroxide nanoplates as high-performance electrocatalyst for oxygen evolution reaction. Applied Clay Science, 2018, 165, 277-283.	5.2	47
96	CoNiFe Layered Double Hydroxide/RuO <sub>2.1</sub> Nanosheet Superlattice as Carbon-Free Electrocatalysts for Water Splitting and Li–O <sub>2</sub> Batteries. ACS Applied Materials & Interfaces, 2020, 12, 33083-33093.	8.0	47
97	Single-Crystal Al18B4O33 Microtubes. Journal of the American Chemical Society, 2002, 124, 10668-10669.	13.7	46
98	Polypyrrole-Modified NH <sub>4</sub> NiPO <sub>4</sub> ·H <sub>2</sub> O Nanoplate Arrays on Ni Foam for Efficient Electrode in Electrochemical Capacitors. ACS Sustainable Chemistry and Engineering, 2016, 4, 5578-5584.	6.7	46
99	Highly Swollen Layered Nickel Oxide with a Trilayer Hydrate Structure. Chemistry of Materials, 2008, 20, 479-485.	6.7	44
100	Recent progress on exploring exceptionally high and anisotropic H <sup>+</sup> /OH <sup>â^'</sup> ion conduction in two-dimensional materials. Chemical Science, 2018, 9, 33-43.	7.4	44
101	Advanced Electrocatalytic Performance of Ni-Based Materials for Oxygen Evolution Reaction. ACS Sustainable Chemistry and Engineering, 2019, 7, 341-349.	6.7	43
102	Simultaneous growth of silicon carbide nanorods and carbon nanotubes by chemical vapor deposition. Chemical Physics Letters, 2002, 354, 264-268.	2.6	42
103	Thermally Stable Luminescent Composites Fabricated by Confining Rare Earth Complexes in the Two-Dimensional Gallery of Titania Nanosheets and Their Photophysical Properties. Journal of Physical Chemistry B, 2006, 110, 9863-9868.	2.6	42
104	Self-Assembled Nanofilm of Monodisperse Cobalt Hydroxide Hexagonal Platelets: Topotactic Conversion into Oxide and Resistive Switching. Chemistry of Materials, 2010, 22, 6341-6346.	6.7	42
105	Hollow spherical rare-earth-doped yttrium oxysulfate: A novel structure for upconversion. Nano Research, 2014, 7, 1093-1102.	10.4	42
106	Room-Temperature Ferromagnetism in Doped Face-Centered Cubic Fe Nanoparticles. Small, 2006, 2, 804-809.	10.0	41
107	Facile Synthesis of Superstructured MoS <sub>2</sub> and Graphitic Nanocarbon Hybrid for Efficient Hydrogen Evolution Reaction. ACS Sustainable Chemistry and Engineering, 2018, 6, 14441-14449.	6.7	41
108	Hybrid Nanostructures of Bimetallic NiCo Nitride/N-Doped Reduced Graphene Oxide as Efficient Bifunctional Electrocatalysts for Rechargeable Zn–Air Batteries. ACS Sustainable Chemistry and Engineering, 2019, 7, 19612-19620.	6.7	41

#	Article	IF	CITATIONS
109	Insights into the critical dual-effect of acid treatment on ZnxCd1-xS for enhanced photocatalytic production of syngas under visible light. Applied Catalysis B: Environmental, 2021, 288, 119976.	20.2	41
110	Thin boron nitride nanotubes with unusual large inner diameters. Chemical Physics Letters, 2001, 350, 434-440.	2.6	39
111	Well-defined crystallites autoclaved from the nitrate/NH4OH reaction system as the precursor for (Y,Eu)2O3 red phosphor: Crystallization mechanism, phase and morphology control, and luminescent property. Journal of Solid State Chemistry, 2012, 192, 229-237.	2.9	39
112	Liquid Phase Exfoliation of MoS <sub>2</sub> Assisted by Formamide Solvothermal Treatment and Enhanced Electrocatalytic Activity Based on (H <sub>3</sub> Mo <sub>12</sub> O <sub>40</sub> P/MoS <sub>2</sub> ) <sub>n</sub> Multilayer Structure. ACS Sustainable Chemistry and Engineering, 2018, 6, 5227-5237.	6.7	39
113	Post-synthesis isomorphous substitution of layered Co–Mn hydroxide nanocones with graphene oxide as high-performance supercapacitor electrodes. Nanoscale, 2019, 11, 6165-6173.	5.6	39
114	Advanced electrocatalysts based on two-dimensional transition metal hydroxides and their composites for alkaline oxygen reduction reaction. Nanoscale, 2020, 12, 21479-21496.	5.6	39
115	Stabilizing CuGaS <sub>2</sub> by crystalline CdS through an interfacial Z-scheme charge transfer for enhanced photocatalytic CO <sub>2</sub> reduction under visible light. Nanoscale, 2020, 12, 8693-8700.	5.6	39
116	Hierarchical CoO/MnCo <sub>2</sub> O <sub>4.5</sub> nanorod arrays on flexible carbon cloth as high-performance anode materials for lithium-ion batteries. Dalton Transactions, 2018, 47, 3775-3784.	3.3	38
117	Liquid dispersions of zeolite monolayers with high catalytic activity prepared by soft-chemical exfoliation. Science Advances, 2020, 6, eaay8163.	10.3	37
118	Construction of a push–pull system in g-C <sub>3</sub> N <sub>4</sub> for efficient photocatalytic hydrogen evolution under visible light. Journal of Materials Chemistry A, 2020, 8, 13299-13310.	10.3	37
119	βâ€cyclodextrin as Lithiumâ€ion Diffusion Channel with Enhanced Kinetics for Stable Silicon Anode. Energy and Environmental Materials, 2021, 4, 72-80.	12.8	36
120	Stability and Nature of Chemically Exfoliated MoS <sub>2</sub> in Aqueous Suspensions. Inorganic Chemistry, 2017, 56, 7620-7623.	4.0	35
121	Two-dimensional porous cuprous oxide nanoplatelets derived from metal–organic frameworks (MOFs) for efficient photocatalytic dye degradation under visible light. Dalton Transactions, 2018, 47, 7694-7700.	3.3	35
122	Activating Hematite Nanoplates via Partial Reduction for Electrocatalytic Oxygen Reduction Reaction. ACS Sustainable Chemistry and Engineering, 2019, 7, 11841-11849.	6.7	35
123	Aluminum Borate–Boron Nitride Nanocables. Advanced Materials, 2003, 15, 1377-1379.	21.0	34
124	Morphological Evolution and Magnetic Property of Rareâ€Earthâ€Doped Hematite Nanoparticles: Promising Contrast Agents for T1â€Weighted Magnetic Resonance Imaging. Advanced Functional Materials, 2017, 27, 1606821.	14.9	34
125	Progress and perspective on two-dimensional unilamellar metal oxide nanosheets and tailored nanostructures from them for electrochemical energy storage. Energy Storage Materials, 2019, 19, 281-298.	18.0	34
126	Structural Study of a Series of Layered Rare-Earth Hydroxide Sulfates. Inorganic Chemistry, 2011, 50, 6667-6672.	4.0	33

#	Article	IF	CITATIONS
127	Novel Route to WOxNanorods and WS2Nanotubes from WS2Inorganic Fullerenes. Journal of Physical Chemistry B, 2006, 110, 18191-18195.	2.6	32
128	Macroscopic and Strong Ribbons of Functionality-Rich Metal Oxides from Highly Ordered Assembly of Unilamellar Sheets. Journal of the American Chemical Society, 2015, 137, 13200-13208.	13.7	32
129	Facile synthesis of porous FeCo2O4 nanowire arrays on flexible carbon cloth with superior lithium storage properties. Journal of Physics and Chemistry of Solids, 2018, 122, 261-267.	4.0	32
130	Synthesis and Substitution Chemistry of Redox-Active Manganese/Cobalt Oxide Nanosheets. Chemistry of Materials, 2018, 30, 1517-1523.	6.7	31
131	<i>In situ</i> growth of metallic Ag <sup>0</sup> intercalated CoAl layered double hydroxides as efficient electrocatalysts for the oxygen reduction reaction in alkaline solutions. Dalton Transactions, 2019, 48, 1084-1094.	3.3	30
132	Tuning Interfacial Active Sites over Porous Mo <sub>2</sub> N-Supported Cobalt Sulfides for Efficient Hydrogen Evolution Reactions in Acid and Alkaline Electrolytes. ACS Applied Materials & Interfaces, 2021, 13, 41573-41583.	8.0	30
133	In–Ni microballs catalyzed growth of dense and highly aligned silica nanowires. Chemical Physics Letters, 2003, 377, 177-183.	2.6	29
134	Interconnected silicon nanoparticles originated from halloysite nanotubes through the magnesiothermic reduction: A high-performance anode material for lithium-ion batteries. Applied Clay Science, 2018, 162, 499-506.	5.2	29
135	Self-Supported Fe-Doped CoP Nanowire Arrays Grown on Carbon Cloth with Enhanced Properties in Lithium-Ion Batteries. ACS Applied Energy Materials, 2019, 2, 406-412.	5.1	29
136	3D Network Binder via In Situ Crossâ€Linking on Silicon Anodes with Improved Stability for Lithiumâ€lon Batteries. Macromolecular Chemistry and Physics, 2020, 221, 1900414.	2.2	29
137	On/Off Boundary of Photocatalytic Activity between Single- and Bilayer MoS <sub>2</sub> . ACS Nano, 2020, 14, 6663-6672.	14.6	29
138	Molecular-Scale Manipulation of Layer Sequence in Heteroassembled Nanosheet Films toward Oxygen Evolution Electrocatalysts. ACS Nano, 2022, 16, 4028-4040.	14.6	29
139	Layered zinc hydroxide nanocones: synthesis, facile morphological and structural modification, and properties. Nanoscale, 2014, 6, 13870-13875.	5.6	28
140	Three-dimensionally interconnected Si frameworks derived from natural halloysite clay: a high-capacity anode material for lithium-ion batteries. Dalton Transactions, 2018, 47, 7522-7527.	3.3	28
141	Serpentine CoxNi3-xGe2O5(OH)4 nanosheets with tuned electronic energy bands for highly efficient oxygen evolution reaction in alkaline and neutral electrolytes. Applied Catalysis B: Environmental, 2020, 260, 118184.	20.2	28
142	Accelerated Ionic and Charge Transfer through Atomic Interfacial Electric Fields for Superior Sodium Storage. ACS Nano, 2022, 16, 4775-4785.	14.6	28
143	General synthetic strategy for high-yield and uniform rare-earth oxysulfate (RE2O2SO4, RE = La, Pr, Nd,) Tj ETQq1	1_0,7843 3.6	14 rgBT /O
	Hierarchical valhâ <sup>C</sup> "chall lavered potaceium pichate for tupad pH dependent photocatalytic		

Hierarchical yolkâ€"shell layered potassium niobate for tuned pH-dependent photocatalytic H<sub>2</sub> evolution. Catalysis Science and Technology, 2017, 7, 1000-1005.

4.1 27

#	Article	IF	CITATIONS
145	Flexible conductive polymer composite materials based on strutted graphene foam. Composites Communications, 2021, 25, 100757.	6.3	27
146	Impact of perovskite layer stacking on dielectric responses in KCa2Nanâ^'3NbnO3n+1â€^(n=3–6) Dion–Jacobson homologous series. Applied Physics Letters, 2010, 96, .	3.3	26
147	Advanced Supercapacitors Based on α-Ni(OH) <sub>2</sub> Nanoplates/Graphene Composite Electrodes with High Energy and Power Density. ACS Applied Energy Materials, 2018, 1, 1496-1505.	5.1	26
148	Synthesis of Co(II)-Fe(III) Hydroxide Nanocones with Mixed Octahedral/Tetrahedral Coordination toward Efficient Electrocatalysis. Chemistry of Materials, 2020, 32, 4232-4240.	6.7	26
149	Superlattice assembly of graphene oxide (GO) and titania nanosheets: fabrication, in situ photocatalytic reduction of GO and highly improved carrier transport. Nanoscale, 2014, 6, 14419-14427.	5.6	25
150	Two-Dimensional Molecular Sheets of Transition Metal Oxides toward Wearable Energy Storage. Accounts of Chemical Research, 2020, 53, 2443-2455.	15.6	25
151	Surface-Modified Two-Dimensional Titanium Carbide Sheets for Intrinsic Vibrational Signal-Retained Surface-Enhanced Raman Scattering with Ultrahigh Uniformity. ACS Applied Materials & Interfaces, 2020, 12, 23523-23531.	8.0	25
152	Formation, Structure, and Structural Properties of a New Filamentary Tubular Form:Â Hollow Conical-Helix of Graphitic Boron Nitride. Journal of the American Chemical Society, 2003, 125, 8032-8038.	13.7	24
153	Donor–Acceptor Nanoensembles Based on Boron Nitride Nanotubes. Advanced Materials, 2007, 19, 934-938.	21.0	24
154	Serpentine Ni <sub>3</sub> Ge <sub>2</sub> O <sub>5</sub> (OH) <sub>4</sub> Nanosheets with Tailored Layers and Size for Efficient Oxygen Evolution Reactions. Small, 2018, 14, e1803015.	10.0	24
155	Efficient Photoinduced Charge Accumulation in Reduced Graphene Oxide Coupled with Titania Nanosheets To Show Highly Enhanced and Persistent Conductance. ACS Applied Materials & Interfaces, 2015, 7, 11436-11443.	8.0	23
156	Core–shell Fe <sub>3</sub> O <sub>4</sub> @SiO <sub>2</sub> @HNbMoO <sub>6</sub> nanocomposites: new magnetically recyclable solid acid for heterogeneous catalysis. Journal of Materials Chemistry A, 2015, 3, 3456-3464.	10.3	23
157	Cobalt iron phosphide nanoparticles embedded within a carbon matrix as highly efficient electrocatalysts for the oxygen evolution reaction. Chemical Communications, 2019, 55, 9212-9215.	4.1	23
158	Synthesis of silicon nanosheets from kaolinite as a high-performance anode material for lithium-ion batteries. Journal of Physics and Chemistry of Solids, 2020, 137, 109227.	4.0	23
159	Nickel Dichalcogenide Hollow Spheres: Controllable Fabrication, Structural Modification, and Magnetic Properties. Chemistry - A European Journal, 2013, 19, 15467-15471.	3.3	22
160	Controllable synthesis of layered Co–Ni hydroxide hierarchical structures for high-performance hybrid supercapacitors. Journal of Physics and Chemistry of Solids, 2016, 88, 8-13.	4.0	22
161	Superionic conduction along ordered hydroxyl networks in molecular-thin nanosheets. Materials Horizons, 2019, 6, 2087-2093.	12.2	22
162	Giant two-dimensional titania sheets for constructing a flexible fiber sodium-ion battery with long-term cycling stability. Energy Storage Materials, 2020, 24, 504-511.	18.0	22

#	Article	IF	CITATIONS
163	Three-in-one cathode host based on Nb <sub>3</sub> O <sub>8</sub> /graphene superlattice heterostructures for high-performance Li–S batteries. Journal of Materials Chemistry A, 2021, 9, 9952-9960.	10.3	22
164	Lithium doped nickel oxide nanocrystals with a tuned electronic structure for oxygen evolution reaction. Chemical Communications, 2021, 57, 6070-6073.	4.1	22
165	Novel BN tassel-like and tree-like nanostructures. Diamond and Related Materials, 2002, 11, 1397-1402.	3.9	21
166	Selective synthesis and magnetic properties of uniform CoTe and CoTe2 nanotubes. Journal of Materials Chemistry, 2010, 20, 7634.	6.7	21
167	Needle-like CoO nanowires grown on carbon cloth for enhanced electrochemical properties in supercapacitors. RSC Advances, 2015, 5, 41627-41630.	3.6	21
168	Perovskite Solar Cell Using a Two-Dimensional Titania Nanosheet Thin Film as the Compact Layer. ACS Applied Materials & Interfaces, 2015, 7, 15117-15122.	8.0	20
169	Large-Scale Preparation, Chemical Exfoliation, and Structural Modification of Layered Zinc Hydroxide Nanocones: Transformation into Zinc Oxide Nanocones for Enhanced Photocatalytic Properties. ACS Sustainable Chemistry and Engineering, 2017, 5, 5869-5879.	6.7	20
170	Hierarchical Nickel Clusters Encapsulated in Ultrathin N-doped Graphitic Nanocarbon Hybrids for Effective Hydrogen Evolution Reaction. ACS Sustainable Chemistry and Engineering, 2019, 7, 15127-15136.	6.7	20
171	Anisotropic fluoride nanocrystals modulated by facet-specific passivation and their disordered surfaces. National Science Review, 2020, 7, 841-848.	9.5	20
172	The formation of graphene–titania hybrid films and their resistance change under ultraviolet irradiation. Carbon, 2012, 50, 4518-4523.	10.3	19
173	Aqueous Formateâ€Based Liâ€CO <sub>2</sub> Battery with Low Charge Overpotential and High Working Voltage. Advanced Energy Materials, 2021, 11, 2101630.	19.5	19
174	Fullerphene Nanosheets: A Bottomâ€Up 2D Material for Singleâ€Carbonâ€Atomâ€Level Molecular Discrimination. Advanced Materials Interfaces, 2022, 9, .	3.7	19
175	Exfoliated Ferrierite-Related Unilamellar Nanosheets in Solution and Their Use for Preparation of Mixed Zeolite Hierarchical Structures. Journal of the American Chemical Society, 2021, 143, 11052-11062.	13.7	18
176	Catalytic growth of carbon nanofibers on a porous carbon nanotubes substrate. Journal of Materials Science Letters, 2000, 19, 1929-1931.	0.5	16
177	β-Ga2O3 nanowires sheathed with boron nitrogen. Chemical Physics Letters, 2003, 367, 219-222.	2.6	16
178	Synthesis of LDH Nanosheets and their Layer-by-Layer Assembly. Recent Patents on Nanotechnology, 2012, 6, 159-168.	1.3	16
179	Facile synthesis and characterization of core-shell structured Ag 3 PO 4 @Hal nanocomposites for enhanced photocatalytic properties. Applied Clay Science, 2017, 141, 132-137.	5.2	16
180	Insight into the structural and electronic nature of chemically exfoliated molybdenum disulfide nanosheets in aqueous dispersions. Dalton Transactions, 2018, 47, 3014-3021.	3.3	16

#	Article	IF	CITATIONS
181	All solid-state lithium–oxygen batteries with MOF-derived nickel cobaltate nanoflake arrays as high-performance oxygen cathodes. Chemical Communications, 2019, 55, 10689-10692.	4.1	16
182	Spatially-controlled porous nanoflake arrays derived from MOFs: An efficiently long-life oxygen electrode. Nano Research, 2019, 12, 2528-2534.	10.4	16
183	Facile synthesis and characterization of halloysite@W18O49 nanocomposite with enhanced photocatalytic properties. Applied Clay Science, 2019, 183, 105319.	5.2	16
184	Composition Tuning of Ultrafine Cobalt-Based Spinel Nanoparticles for Efficient Oxygen Evolution. ACS Sustainable Chemistry and Engineering, 2020, 8, 5534-5543.	6.7	16
185	General Synthesis of Layered Rare-Earth Hydroxides (RE = Sm, Eu, Gd, Tb, Dy, Ho, Er, Y) and Direct Exfoliation into Monolayer Nanosheets with High Color Purity. Journal of Physical Chemistry Letters, 2021, 12, 10135-10143.	4.6	16
186	Revealing the illumination effect on the discharge products in highâ€performance Li–O <sub>2</sub> batteries with heterostructured photocatalysts. , 2022, 4, 1169-1181.		16
187	The Development of Carbon Nanotubes/RuO2·xH2O Electrodes for Electrochemical Capacitors. Bulletin of the Chemical Society of Japan, 2000, 73, 1813-1816.	3.2	15
188	Pyrolytic-grown B–C–N and BN nanotubes. Science and Technology of Advanced Materials, 2003, 4, 403-407.	6.1	15
189	Elastic deformation of helical-conical boron nitride nanotubes. Journal of Chemical Physics, 2003, 119, 3436-3440.	3.0	15
190	Graphene oxide/titania hybrid films with dual-UV-responsive surfaces of tunable wettability. RSC Advances, 2012, 2, 10829.	3.6	15
191	Highly Enhanced and Switchable Photoluminescence Properties in Pillared Layered Hydroxides Stabilizing Ce <sup>3+</sup> . Journal of Physical Chemistry C, 2015, 119, 26229-26236.	3.1	15
192	Layered rare-earth hydroxide nanocones with facile host composition modification and anion-exchange feature: topotactic transformation into oxide nanocones for upconversion. Nanoscale, 2017, 9, 8185-8191.	5.6	15
193	Monolayer Attachment of Metallic MoS <sub>2</sub> on Restacked Titania Nanosheets for Efficient Photocatalytic Hydrogen Generation. ACS Applied Energy Materials, 2018, 1, 6912-6918.	5.1	15
194	Superlattice films of semiconducting oxide and rare-earth hydroxide nanosheets for tunable and efficient photoluminescent energy transfer. Nanoscale, 2021, 13, 4551-4561.	5.6	15
195	Double Confined MoO <sub>2</sub> /Sn/NC@NC Nanotubes: Solid–Liquid Synthesis, Conformal Transformation, and Excellent Lithium-Ion Storage. ACS Applied Materials & Interfaces, 2021, 13, 19836-19845.	8.0	15
196	Chemically exfoliated inorganic nanosheets for nanoelectronics. Applied Physics Reviews, 2022, 9, .	11.3	15
197	Controlled fabrication and optical properties of uniform CeO2 hollow spheres. RSC Advances, 2013, 3, 3544.	3.6	14

New Family of Lanthanide-Based Inorganic–Organic Hybrid Frameworks: Ln<sub>2</sub>(OH)<sub>4</sub>[O<sub>3</sub>S(CH<sub>2</sub>)<sub><i>n</i></sub>SO<sub>3</sub>]Â42H<sub>24K/sub>O (Ln = La, Ce, Pr, Nd, Sm; <i>n</i> = 3, 4) and Their Derivatives. Inorganic Chemistry, 2013, 52, 1755-1761. 198

#	Article	IF	CITATIONS
199	Controllable Fabrication of Rare-Earth-Doped Gd <sub>2</sub> O <sub>2</sub> SO <sub>4</sub> @SiO <sub>2</sub> Double-Shell Hollow Spheres for Efficient Upconversion Luminescence and Magnetic Resonance Imaging. ACS Sustainable Chemistry and Engineering, 2018, 6, 10463-10471.	6.7	14
200	Ag1.69Sb2.27O6.25 coupled carbon nitride photocatalyst with high redox potential for efficient multifunctional environmental applications. Applied Surface Science, 2019, 487, 82-90.	6.1	14
201	Binder-Free Co <sub>4</sub> N Nanoarray on Carbon Cloth as Flexible High-Performance Anode for Lithium-Ion Batteries. ACS Applied Energy Materials, 2018, 1, 4432-4439.	5.1	13
202	Acetate-induced controlled-synthesis of hematite polyhedra enclosed by high-activity facets for enhanced photocatalytic performance. RSC Advances, 2016, 6, 66879-66883.	3.6	12
203	Ultrathin Nanosheet-Assembled Co–Fe Hydroxide Nanotubes: Sacrificial Template Synthesis, Topotactic Transformation, and Their Application as Electrocatalysts for Efficient Oxygen Evolution Reaction. ACS Applied Materials & Interfaces, 2020, 12, 46578-46587.	8.0	12
204	Construction of Multilayer Films and Superlattice- and Mosaic-like Heterostructures of 2D Metal Oxide Nanosheets via a Facile Spin-Coating Process. ACS Applied Materials & Interfaces, 2021, 13, 43258-43265.	8.0	12
205	Photo-irradiation tunes highly active sites over β-Ni(OH) <sub>2</sub> nanosheets for the electrocatalytic oxygen evolution reaction. Chemical Communications, 2021, 57, 9060-9063.	4.1	12
206	Activity enhancement of layered cobalt hydroxide nanocones by tuning interlayer spacing and phosphidation for electrocatalytic water oxidation in neutral solutions. Inorganic Chemistry Frontiers, 2019, 6, 1744-1752.	6.0	11
207	Self-assembled array of boron oxide nanowires on Mg surface. Chemical Physics Letters, 2003, 374, 358-361.	2.6	10
208	Hydrothermal synthesis of three-dimensional core-shell hollow N-doped carbon encapsulating SnO2@CoO nanospheres for high-performance lithium-ion batteries. Materials Today Energy, 2019, 14, 100354.	4.7	10
209	Luminescent Yttrium Oxide Nanosheets for Temperature Sensing. ACS Applied Nano Materials, 2021, 4, 12316-12324.	5.0	10
210	Patterned Nanowires of Se and Corresponding Metal Chalcogenides from Patterned Amorphous Se Nanoparticles. Small, 2009, 5, 356-360.	10.0	9
211	Self-Assembled Corn-Husk-Shaped Fullerene Crystals as Excellent Acid Vapor Sensors. Chemosensors, 2022, 10, 16.	3.6	9
212	Fabrication and Electrochemical Characterization of Molecularly Alternating Self-Assembled Films and Capsules of Titania Nanosheets and Gold Nanoparticles. Current Nanoscience, 2007, 3, 155-160.	1.2	7
213	Dendritic Silica Nanoparticles Synthesized by a Block Copolymer-Directed Seed-Regrowth Approach. Langmuir, 2015, 31, 1610-1614.	3.5	7
214	Massive hydration-driven swelling of layered perovskite niobate crystals in aqueous solutions of organo-ammonium bases. Dalton Transactions, 2018, 47, 3022-3028.	3.3	7
215	Rare-earth-doped yttrium oxide nanoplatelets and nanotubes: controllable fabrication, topotactic transformation and upconversion luminescence. CrystEngComm, 2018, 20, 5025-5032.	2.6	7
216	Formation of nano-sized particles of a solid electrolyte by laser ablation. Journal of Power Sources, 2005, 146, 703-706.	7.8	6

#	Article	IF	CITATIONS
217	Alternate Restacking of 2 D CoNi Hydroxide and Graphene Oxide Nanosheets for Energetic Oxygen Evolution. ChemSusChem, 2019, 12, 5274-5281.	6.8	6
218	Photocharge Trapping in Two-Sheet Reduced Graphene Oxide–Ti <sub>0.87</sub> O <sub>2</sub> Heterostructures and Their Photoreduction and Photomemory Applications. ACS Applied Nano Materials, 2019, 2, 6378-6386.	5.0	6
219	Preparation of 1D ultrathin niobate nanobelts by liquid exfoliation as photocatalysts for hydrogen generation. Chemical Communications, 2019, 55, 2417-2420.	4.1	6
220	Heterostructured NiFe oxide/phosphide nanoflakes for efficient water oxidation. Dalton Transactions, 2019, 48, 8442-8448.	3.3	6
221	Multi-shelled cobalt–nickel oxide/phosphide hollow spheres for an efficient oxygen evolution reaction. Dalton Transactions, 2020, 49, 10918-10927.	3.3	6
222	Electronic configuration modulation of tin dioxide by phosphorus dopant for pathway change in electrocatalytic water oxidation. Inorganic Chemistry Frontiers, 2021, 9, 83-89.	6.0	5
223	Silicon nanosheets derived from silicate minerals: controllable synthesis and energy storage application. Nanoscale, 2021, 13, 18410-18420.	5.6	3
224	Terbiumâ€Doped Layered Yttrium Hydroxide Nanocone: Controlled Synthesis, Structure Variations, Phase Conversion to Oxide/Oxysulfate Nanocone and Their Luminescence Properties. Particle and Particle Systems Characterization, 2018, 35, 1800075.	2.3	2
225	Controllable fabrication of graphitic nanocarbon encapsulating FexNiy hybrids for efficient splitting of water. Journal of Alloys and Compounds, 2020, 829, 154421.	5.5	2
226	Tb <sup>3+</sup> /Sm <sup>3+</sup> co-doped double perovskite: synthesis, exfoliation and luminescence properties. Chemical Communications, 2022, 58, 6626-6629.	4.1	2